JOURNAL OF THEORETICAL AND APPLIED MECHANICS
47, 4, pp. xx-yy, Warsaw 2009

MICROMECHANICAL MODEL OF AUXETIC CELLULAR MATERIALS

Małgorzata Janus-Michalska

Cracow University of Technology, Institute of Structural Mechanics, Cracow, Poland
e-mail: mjm@limba.wil.pk.edu.pl

An effective anisotropic continuum formulation for auxetic cellular materials is the objective of this paper. A skeleton is modelled as a plane beam elastic structure with stiff joints. The skeleton topology, forming concave polygons, is responsible for negative Poisson's ratio effect. The essential macroscopic features of mechanical behaviour are inferred from the deformation response of a representative volume element using the framework of micromechanical analysis. The strain energy of a unit cell is calculated by adding the tensile, shearing and bending strain energy of individual members. The equivalent continuum is based on averaging this energy, thus formulating the basis for computing the anisotropic stiffness matrix. The structural mechanics methodology and ANSYS finite element code are applied to solve the beam model of the skeleton. Graphical representation of certain material constants such as Young's modulus, Poisson's ratio, shear modulus and generalized bulk modulus is given. The results of included parametric study may be used for proper choice of geometric and material data of the skeleton for a given structural application of the anisotropic continuum.

Key words: auxetic cellular materials, anisotropy, effective model, elasticity

1. Introduction

Auxetic materials are of interest because of enhanced material properties related to negative Poisson's ratio. Such materials are called also dilatational materials because they exhibit substantial volumetric changes when loaded. First auxetic cellular structures were created as 2D silicone rubber or aluminum honeycombs and were extensively investigated by Lakes (1991-1993), Lakes *et al.* (1988), Lakes and Witt (2002). Materials with negative Poisson's ratio are more resilient than non-auxetic materials, and the linear strain-stress relationship can reach up to 0.40 compressive ultimate strain compared to 0.05 strain for conventional cellular materials. Auxetic materials also exhibit lower

stiffness and greater resistance to indentations than ordinary materials. This property may be useful in certain applications such as matresses and wrestling mats. Auxetic materials better redistribute strain under external loads. Negative Poisson's ratio may significantly influence stress distribution in contact problems, reduce stress concentrations, substantially affect the Saint Venant effect and yield double curvature effect in 3D bending problems. This novel behaviour is important in design considerations. An increasing number of materials and processing routines are developed and tailored to specific applications. Auxetic behaviour can be described by classical theory of elasticity and it does not depend on scale (Lakes, 1991b). Deformation takes place on the micro or macro level. This means that one may consider auxetic matrials as well as auxetic structures.

Physical origin of mechanical behaviour of cellular materials is based on structural considerations. Structural analysis of a skeleton on the micro level explains macroscopic behaviour of such structured bodies. The overall effective properties are determined by considerations using transition between micro and macro scales of observation. This corresponds to effective model construction (Hori and Nemet-Naser, 1999; Nemat-Naser and Hori, 1999). The effective properties are then used to determine the response of structural elements on the macro scale and emerge naturally as a consequence of micro-macro relations without depending on specific physical measurements on the macroscopic level (Nemat-Naser and Hori, 1999). This method, typical for micromechanics, has been applied to aluminum foams Janus-Michalska and Pęcherski (2003), and a group of 3D cellular structures forming positive Poisson's ratio cellular materials Janus-Michalska (2005). The existing solutions concerning stiffness matrices for auxetic cellular materials are mainly based on the homogenization approach (Kumar and McDowell, 2004). The most recent solution for auxetic structures is the missing ribs method by Smith *et al.* (2000).

The approach based on micromechanical modelling presented in this paper is advantageous because the dependence of effective properties on microstructural parameters is easily readable here. Thus structural topology and skeleton material may be properly chosen in order to obtain the required properties of the cellular material.

2. Micromechanical analysis

A micromechanical framework similar to that proposed in Janus-Michalska and Pęcherski (2003), Janus-Michalska (2005) has been developed to determine equivalent continuum properties. The internal structure of a material is

assumed to be periodical one, and is the basis for studying overall mechanical properties of a cellular auxetic material.

2.1. Representative unit cell

A theoretical investigation is conducted for a material exhibiting two the dimensional reentrant hexagonal microstructure as shown in Fig. 1a.

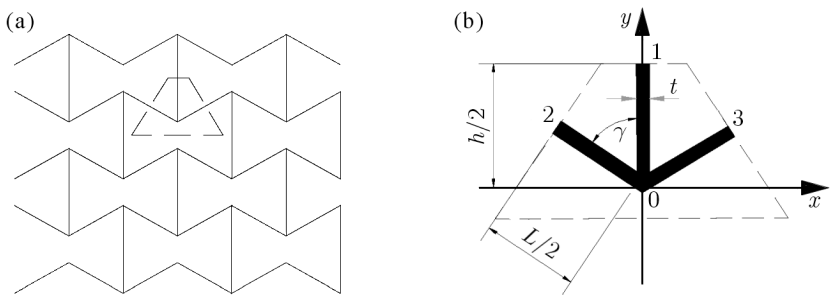

Fig. 1. A cellular structure and a representative unit cell

Formulation on the micro level begins by identifying the unit cell of the spatially periodic array. The idea adopted here is based on the fact that the essential feature of arbitrary uniform deformation of the whole beam structure is affinity of midpoint displacements (Waren and Kraynik, 1988; Janus-Michalska and Pęcherski, 2003). It results in the same structural response of parts of the skeleton consisting of the node and halves of beams. The representative unit cell defined as the smallest part of the skeleton with repetitive response was successively applied to foams (Janus-Michalska and Pęcherski, 2003), and 3D periodic cellular structures (Janus-Michalska, 2005). The detailed description of unit cell construction is given in Janus-Michalska (2005).

The cell corresponding to the reentrant hexagonal structure is given in Fig. 1b. The skeleton of the cell is modelled as an elastic beam structure with a stiff joint (vertex 0). The strut midpoints are described by the position vectors

$$\boldsymbol{b}_1^0 = \Big(0, \frac{h}{2}\Big) \qquad \boldsymbol{b}_2^0 = \Big(\frac{L}{2}\sin\gamma, \frac{L}{2}\cos\gamma\Big) \qquad \boldsymbol{b}_3^0 = \Big(-\frac{L}{2}\sin\gamma, \frac{L}{2}\cos\gamma\Big)$$

where: $|\boldsymbol{b}_1^0| = h/2$, $|\boldsymbol{b}_2^0| = L/2$, $|\boldsymbol{b}_3^0| = L/2$. Beam lengths and γ angle should satisfy the following conditions, which are necessary to obtain the representative volume element (RVE) shown by the dotted line in Fig. 1a: $L\cos\gamma \leqslant h/2$ and $\cos\gamma \leqslant L/h$.

The thickness of RVE is assumed to be $H = 1$ in the direction perpendicular to the (x, y) plane. The volume of the unit cell is

$$V = [(h - L\cos\gamma)L\sin\gamma]H$$

Three surfaces of RVE perpendicular to struts i, where $i = 1, 2, 3$ are considered for further calculations, and they are computed as follows

$$A_1 = \Big(\frac{L - h\cos\gamma}{\sin\gamma}\Big)H \qquad A_2 = A_3 = \Big(\frac{h - L\cos\gamma}{\sin\gamma}\Big)H$$

The part of the skeleton included in RVE consists of beams of rectangular cross-sections $A_s = tH$, where t denotes beam thickness. The skeleton volume is thus determined as: $V_s = (L + h/2)tH$. The cellular material may be characterised by its relative density: $\rho^* = \rho/\rho_s$, where ρ and ρ_s denote the cellular material and skeleton material densities, respectively. The relative density may be expressed by relation

$$\rho^* = \frac{\Big(L + \frac{h}{2}\Big)t}{(h - L\cos\gamma)L\sin\gamma}$$

The structure is specified by four geometric structural parameters: L, h, t, γ. Three material parameters: R_e^s – yield stress, E_s – Young's modulus, ν_s – Poisson's ratio must be given to describe the skeleton material.

On the basis of the unit cell model, effective properties of cellular material can be derived.

2.2. Uniform strains for linear elasticity

Uniform plain deformation of a solid with repetitive microstructure results in displacement affinity (Janus-Michalska, 2005). Periodic skeleton structure requires that the individual beams deform antisymmetrically about their midpoints, so the resultant forces at each midpoint reduce to axial and transversal force (Janus-Michalska, 2005) (resultant bending moment at the midpoint vanishes).

In micromechanics, strains are defined as volumetric averages of the micro field variables (Nemat-Naser and Hori, 1999) and read as follows

$$\boldsymbol{\varepsilon} = \langle \boldsymbol{\varepsilon}^s \rangle_V = \frac{1}{V}\sum_{A_i} sym(\boldsymbol{n}_i \otimes \boldsymbol{u}_i)\, dS \tag{2.1}$$

where: $\langle\cdot\rangle_V$ stands for the volumetric average in the skeleton s taken over V, $\boldsymbol{n}_i$ is the outer unit normal on the boundary $\boldsymbol{n}_i = \boldsymbol{b}_1^0/|\boldsymbol{b}_i^0|$, $\boldsymbol{u}_i$ – the midpoint displacement on the surface A_i.

Three independent uniform unit deformations ${}^{K}\widetilde{\varepsilon}$, described by the following strain vector components (Kelvin's notation in 6-D space) are considered

$$ {}^{1}\widetilde{\varepsilon} = \varepsilon_x = 1 \qquad {}^{2}\widetilde{\varepsilon} = \varepsilon_y = 1 \qquad {}^{3}\widetilde{\varepsilon} = \sqrt{2}\varepsilon_{xy} = 1 \tag{2.2} $$

This results in the following midpoint displacements:
— for uniaxial extensions

$$ \boldsymbol{\Delta}_i({}^{1}\widetilde{\varepsilon}) = {}^{1}\widetilde{\varepsilon}(\boldsymbol{b}_i^0 \cdot \boldsymbol{e}_x)\boldsymbol{e}_x \qquad \boldsymbol{\Delta}_i({}^{2}\widetilde{\varepsilon}) = {}^{2}\widetilde{\varepsilon}(\boldsymbol{b}_i^0 \cdot \boldsymbol{e}_y)\boldsymbol{e}_y \qquad i = 1,2,3 \tag{2.3} $$

— for pure shear

$$ \boldsymbol{\Delta}_i({}^{3}\widetilde{\varepsilon}) = {}^{3}\widetilde{\varepsilon}[(\boldsymbol{b}_i^0 \cdot \boldsymbol{e}_x)\boldsymbol{e}_y + (\boldsymbol{b}_i^0 \cdot \boldsymbol{e}_y)\boldsymbol{e}_x \qquad i = 1,2,3 \tag{2.4} $$

where $\boldsymbol{e}_x$, $\boldsymbol{e}_y$ are unit vectors parallel to the x, y axes.

2.3. Mechanical model of cellular skeleton structure

A typical microstructure skeleton consists of thick beams, which may be described by the Timoshenko beam model. For structures consisting of long slender beams, thus yielding low relative cellular material density, the Bernoulli-Euler beam model is sufficient. Structural mechanics methods are used to analyse the skeleton structure. Resultant forces, i.e. normal force, tangent force and bending moment for the sets of midpoint displacements given by Eqs. (2.3) and (2.4), related to uniform deformation, are obtained by making use of the ANSYS FEM code. The skeleton part within the RVE is therefore as shown as in Fig. 2.

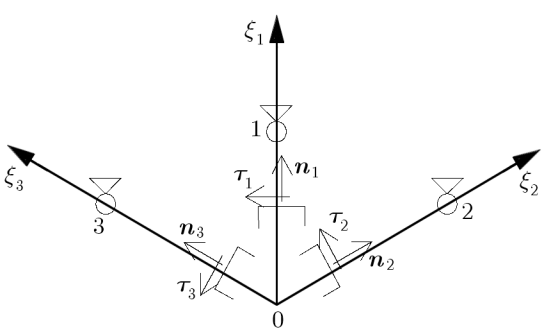

Fig. 2. A part of the skeleton with the stiff node 0 and a local beam system of coordinates

The following notation is used:

ξ_i – local coordinate axis for strut i, $\xi_i(0) = 0$, $0 \leqslant \xi_i \leqslant l_i$, $l_i = h/2$ for $i = 1$, $l_i = L/2$ for $i = 2,3$

$\boldsymbol{n}_i$ – versor normal to the i-th beam cross-section
$\boldsymbol{\tau}_i$ – versor tangent to the i-th beam cross-section.

The axial and transversal force functions are constant along the beam axes, while the bending moment changes linearly as follows

$$\begin{aligned} &{}^K\widetilde{F}_{ni}(\xi_i) = {}^K\widetilde{F}_{ni} && {}^K\widetilde{F}_{\tau i}(\xi_i) = {}^K\widetilde{F}_{\tau i} \\ &{}^K\widetilde{M}_i(\xi_i) = {}^K\widetilde{F}_{\tau i}(l_i - \xi_i) && K = 1,2,3 \qquad i = 1,2,3 \end{aligned} \tag{2.5}$$

Due to linearity of the problem, superposition is possible, and thence for an arbitrary strain state $\boldsymbol{\varepsilon} = ({}^1\varepsilon, {}^2\varepsilon, {}^3\varepsilon)$, the forces are a linear combination of solutions computed for unit strains and read as follows

$$F_{ni}(\boldsymbol{\varepsilon}) = \sum_{K=1}^{3} {}^K\varepsilon {}^K\widetilde{F}_{ni} \qquad F_{\tau i}(\boldsymbol{\varepsilon}) = \sum_{K=1}^{3} {}^K\varepsilon {}^K\widetilde{F}_{\tau i} \tag{2.6}$$

2.4. Equivalent continuum based on averaging of strain potential

The approach adopted here is based on equivalence of the strain potential for the discrete structure and the strain potential of an effective continuum. It refers to averaging the strain energy density (Nemat-Naser and Hori, 1999) as written below

$$\Phi_E = \langle {}^s\Phi_E \rangle_V = \frac{1}{V} \int_{V_s} ({}^s\Phi_E)\, dV_s \tag{2.7}$$

The strain potential of the beam skeleton may be obtained using the following formula (Piechnik, 2003)

$$U = \int_{V_s} ({}^s\Phi_E)\, dV_s = \sum_{i=1}^{3} \left(\int_0^{l_i} \frac{(F_{ni})^2\, d\xi_i}{2E_s A_s} + \mu \int_0^{l_i} \frac{(F_{\tau i})^2\, d\xi_i}{2G_s A_s} + \int_0^{l_i} \frac{[F_{\tau i}(l_i - \xi_i)]^2\, d\xi_i}{2E_s J} \right) \tag{2.8}$$

where

E_s, G_s – Young's and shear modulus for the skeleton material
A_s, J – beam cross-sectional area and moment of inertia
μ – energy cross-sectional coefficient (for rectangular cross-section $\mu = 1.2$).

Due to linearity of the stress-strain relationship, the strain energy density function is represented by the following quadratic form

$$\Phi_E = \frac{1}{2} \boldsymbol{\varepsilon} : \mathbf{S} : \boldsymbol{\varepsilon} \tag{2.9}$$

For simplicity, it is convenient to express strains, stresses and stiffness matrix in terms of 6D space (Kelvin notation), where the plane stress tensor is represented by a vector and the stiffness tensor representation is a 3×3 matrix.

Introducing relation (2.6) to the expression of strain potential and differentiating with respect to strain components as follows

$$S_{IJ} = \frac{1}{V} \frac{\int\limits_{V_s} \partial^2({}^s\Phi_E)}{\partial({}^I\varepsilon)\partial({}^J\varepsilon)} \tag{2.10}$$

one obtains the following formula for stiffness matrix components

$$S_{IJ} = \frac{1}{V} \sum_{i=1}^{3} \Big[\frac{l_i}{E_s A} {}^I\widetilde{F}_{in} {}^J\widetilde{F}_{in} + \Big(\frac{\mu l_i}{G_s A} + \frac{l_i^3}{3E_s J} \Big) {}^I\widetilde{F}_{i\tau} {}^J\widetilde{F}_{i\tau} \Big] \qquad I, J = 1, 2, 3 \tag{2.11}$$

It is worth to emphasise that the energy based definition of $\mathbf{S}$ in general does not lead to the same quantities as those obtained through the stress-strain relations based on averaging of stresses in the skeleton over volume of the representative cell (Janus-Michalska, 2005; Nemat-Naser and Hori, 1999).

The stiffness matrix for the considered type of symmetry is as follows

$$\mathbf{S} = \begin{bmatrix} S_{11} & S_{12} & 0 \\ S_{12} & S_{22} & 0 \\ 0 & 0 & S_{33} \end{bmatrix} \tag{2.12}$$

Its zero components result from the distribution of resultant forces ${}^K\widetilde{F}_{ni}$, ${}^K\widetilde{F}_{\tau i}$ in the skeleton. Those forces are symmetrical for $K = 1, 2$ and antisymmetrical for $K = 3$.

The constitutive relation for the equivalent continuum is determined by the following linear relation

$$\boldsymbol{\sigma} = \mathbf{S} : \boldsymbol{\varepsilon} \tag{2.13}$$

2.5. Anisotropic linear properties

Anisotropic properties are represented by a stiffnes matrix or by a directional distribution of stiffness moduli. For plane structures, the direction is represented by the vector $\boldsymbol{n}$ shown in Fig. 3, defined through the angle θ measured from the axis $\boldsymbol{x}$ of the cell coordinate system to the direction $\boldsymbol{n}$.

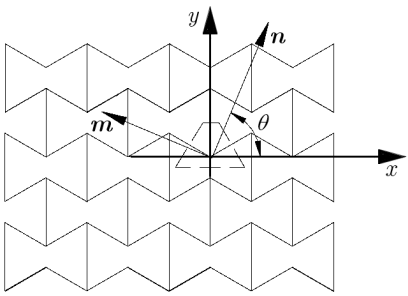

Fig. 3. Directions $\boldsymbol{n}$, $\boldsymbol{m}$ with respect to the cell coordinate system

The following stiffness moduli are considered: Young's modulus $E(\boldsymbol{n})$, Poisson's ratio $\nu(\boldsymbol{n},\boldsymbol{m})$, shear modulus $G(\boldsymbol{n},\boldsymbol{m})$, generalized bulk modulus $K(\boldsymbol{n})$. They can be obtained using the following definitions

$$\begin{aligned}
&\frac{1}{E(\boldsymbol{n})} = (\boldsymbol{n}\otimes\boldsymbol{n})\cdot\mathbf{C}\cdot(\boldsymbol{n}\otimes\boldsymbol{n})\\
&\frac{-\nu(\boldsymbol{n},\boldsymbol{m})}{E(\boldsymbol{n})} = (\boldsymbol{n}\otimes\boldsymbol{n})\cdot\mathbf{C}\cdot(\boldsymbol{m}\otimes\boldsymbol{m})\\
&\frac{1}{2G(\boldsymbol{n},\boldsymbol{m})} = (\boldsymbol{n}\otimes\boldsymbol{m})\cdot\mathbf{C}\cdot(\boldsymbol{n}\otimes\boldsymbol{m})\Big)\\
&\frac{1}{3K(\boldsymbol{n})} = \mathbf{I}\cdot\mathbf{C}\cdot(\boldsymbol{n}\otimes\boldsymbol{n})
\end{aligned} \tag{2.14}$$

where

- $\boldsymbol{n}$ – versor specifying the tensile direction in a tension test
- $\boldsymbol{m}$ – versor perpendicular to the direction of tension $\boldsymbol{n}$
- $\mathbf{C}=\mathbf{S}^{-1}$ – compliance tensor
- $\mathbf{I}$ – unit tensor
- $\boldsymbol{n}\otimes\boldsymbol{n}, \boldsymbol{n}\otimes\boldsymbol{m}$ – diadic tensors.

In Kelvin's notation, the diadics and tensors have the representation given below

$$\begin{aligned}
&\boldsymbol{n}\otimes\boldsymbol{n} = \Big(\cos^2\theta, \sin^2\theta, \frac{1}{\sqrt{2}}\cos\theta\sin\theta\Big)\\
&\boldsymbol{n}\otimes\boldsymbol{m} = \Big(-\cos\theta\sin\theta, \cos\theta\sin\theta, \frac{1}{\sqrt{2}}(\cos^2\theta-\sin^2\theta)\Big)\\
&\mathbf{I} = (1,1,0) \qquad\qquad \mathbf{C} = \begin{bmatrix} C_{11} & C_{12} & 0\\ C_{12} & C_{22} & 0\\ 0 & 0 & C_{33}\end{bmatrix}
\end{aligned} \tag{2.15}$$

The anisotropy parameters defined as follows

$$J_1 = \frac{S_{11}}{S_{22}} \qquad J_2 = \frac{S_{12} + 2S_{33}}{S_{11}}$$

are introduced to measure the degree of anisotropy (for isotropy $J_1 = J_2 = 1$).

3. Examples

3.1. Comparison with results available in literature

The effective elastic stiffness matrix $\mathbf{S}$ calculated according to the proposed method is compared with the matrix $\mathbf{S}*$ available in literature (Overaker *et al.*, 1998) for the following geometrical data: $L = 3.152\,\text{mm}$, $h = 3.152\,\text{mm}$, $t = 0.15\,\text{mm}$, $\gamma = 70°$, thus yielding the material of relative density $\rho/\rho_s = 0.1155$. Skeleton material data are: $E_s = 10\,\text{GPa}$, $\nu_s = 0.3$, ${}^sR_e = 100\,\text{MPa}$.

The computed values

$$\mathbf{S}* = \begin{bmatrix} 73.112 & -18.49 & 0 \\ 0 & 4.804 & 0 \\ 0 & 0 & 0.038 \end{bmatrix} \cdot \text{kPa} \qquad \mathbf{S} = \begin{bmatrix} 73.122 & -18.489 & 0 \\ 0 & 4.803 & 0 \\ 0 & 0 & 0.038 \end{bmatrix} \cdot \text{kPa}$$

show that application of both methods leads to similar results.

3.2. Structural modelling and obtained material properties

Geometric parameters of the skeleton structure are chosen to satisfy the assumptions of the Timoshenko beam theory (beams are not overly thick) and to avoid buckling (beams are not overly slender).

Calculations are performed for the material data as in the previous example and geometric parameters given in Table 1.

The obtained effective stiffness moduli and anisotropy coefficients for the given structures are put together in Table 2.

The dependence of stiffness moduli on the angle θ yields plots presented in Figs. 4-7. The plots are given for angles $0° \leqslant \theta \leqslant 180°$ (for $180° \leqslant \theta \leqslant 360°$ the plots are the same).

The analysis shows that cell shape (ratio L/h and angle γ) determines the type of anisotropy and plots shapes. Comparison of these plots leads to conclusion that for materials of identical cell shapes (structure (2) and (6)), which result in similar anisotropy parameters, the curves $E(\theta)$, $G(\theta)$, $K(\theta)$

Table 1. Geometric parameters

Structure type	L [mm]	h [mm]	γ [–]	t [mm]	$\min\left\{\frac{L}{t}, \frac{h}{t}\right\}$	$\max\left\{\frac{L}{t}, \frac{h}{t}\right\}$
(1)	1.50	1.50	80°	0.15	10.0	10.0
(2)	1.50	2.00	60°	0.15	10.0	13.33
(3)	1.50	3.00	80°	0.15	10.0	20.0
(4)	3.00	1.40	80°	0.15	9.333	20.0
(5)	1.50	3.00	60°	0.15	20.0	20.0
(6)	3.00	4.00	60°	0.15	20.0	26.67

Table 2. Stiffness moduli and anisotropy coefficients

Structure type	E_X [kPa]	E_Y [kPa]	ν_{XY}	ν_{YX}	$\max\left(\frac{G}{K}\right)$	J_1	J_2
(1)	46.183	1.297	−5.058	−0.142	5.52	35.556	−0.1317
(2)	6.270	1.941	−1.718	−0.532	28.9	3.230	−0.5192
(3)	20.900	2.808	−2.289	−0.307	10.1	7.442	−0.2996
(4)	20.071	0.0586	−17.708	−0.0527	14.4	342.07	−0.0495
(5)	3.6713	3.4074	−0.9823	−0.9119	108.3	1.0774	−0.8970
(6)	0.7834	0.2402	−1.786	−0.5472	34.2	3.1616	−0.5448

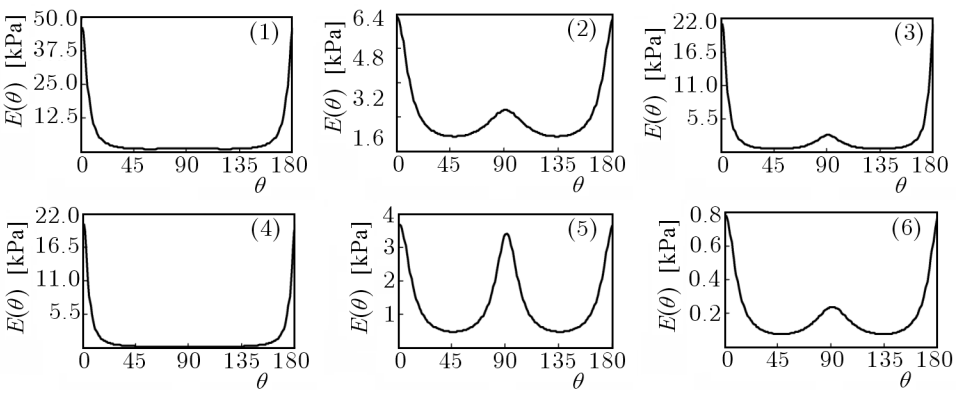

Fig. 4. Young's modulus in dependence of the angle θ for different structures

are also similar and their maximum values decrease approximately with the third power of dimension of the proportion ratio. This phenomenon may be explained by domination of bending over tension in skeleton beams, resulting in such a dependence (Janus-Michalska, 2005). Materials with slender skeleton beams are very compliant.

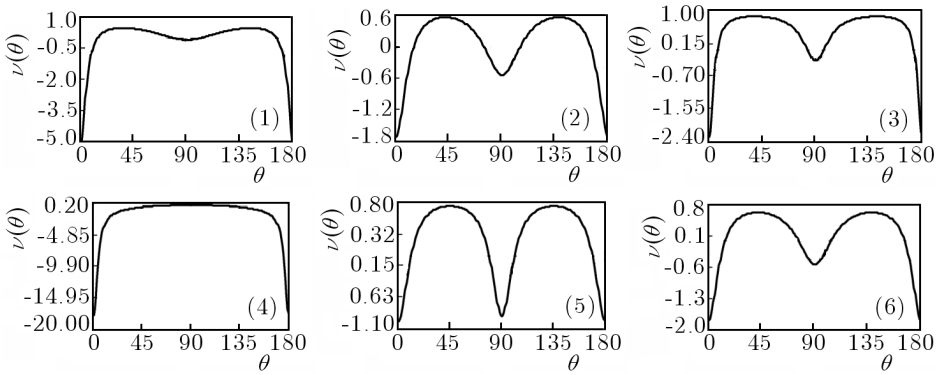

Fig. 5. Poisson's ratio in dependence of the angle θ for different structures

For anisotropic materials the bounds of negative Poisson's ratio are wider than for isotropic materials, and theoreticaly may reach infinity (for isotropic materials in two-dimensional problems the acceptable Poisson's ratio is limited by $-1 \leqslant \nu \leqslant 1$). The existence of directions with high auxetic behaviour in cellular materials is bound with high anisotropy (both parameters influence the plot shape).

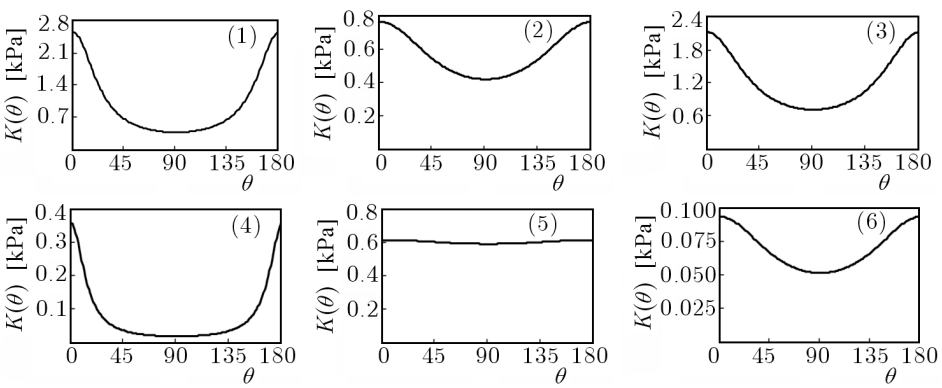

Fig. 6. Generalized bulk modulus in dependence of the angle θ for different structures

The quantity $1/[3K(\theta)]$ represents the relative change of volume per tensile unit stress in the direction given by θ. The bulk modulus is sensitive only to the first anisotropy parameter J_1.

Contrary to the bulk modulus K, shear modulus G is only sensitive to the second anisotropy parameter J_2.

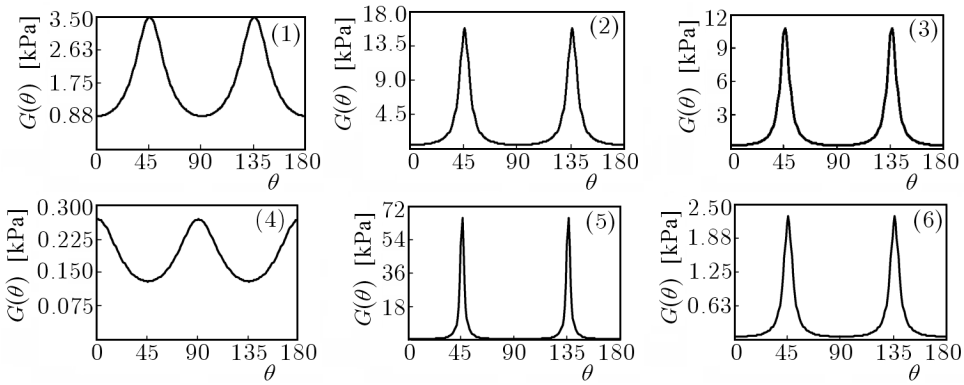

Fig. 7. Shear modulus in dependence of the angle θ for different structures

Due to lack of typical symmetry, the distribution of stiffness moduli depends only on the choice of geometric and material parameters, which results in various anisotropy parameters and values of stiffness moduli.

4. Conclusions

An effective model based on the framework of micromechanical analysis is built and applied for an auxetic cellular material to predict elastic properties on the macroscale. The same framework can be applied for arbitrary cellular material with open cells of a regular skeleton structure. It is especially useful for cells representing complicated shapes of the skeleton (multiple nodes, lack of symmetry). Various structural topologies of cellular materials and skeleton materials result in different macroscopic properties, which can be tailored to special demands. The proper choice of microstructural geometrical parameters determines expected elastic properties. The sensitivity analysis of structural parameters for the auxetic cellular material allows for formulation of modelling indications.

References

1. Gibson L.J., Ashby M.F., 1997, *Cellular Solids*, 2nd edition, Cambridge University Press
2. Hori M., Nemat-Nasser S., 1999, On micromechanics theories for determining micro-macro relations in heterogeneous solids, *Mechanics of Materials*, **31**, 667-682

3. JANUS-MICHALSKA M., 2005, Effective models describing elastic behaviour of cellular materials, *Archives of Metallurgy and Materials*, **50**, 3, 596-608

4. JANUS-MICHALSKA M., PĘCHERSKI R.B., 2003, Macroscopic properties of open-cell foams based on micromechanical modelling, **Technische Mechanik**, **23**, 2/4

5. KORDZIKOWSKI P., JANUS-MICHALSKA M., PĘCHERSKI R.B., 2005, Specification of energy-based criterion of elastic limit states for cellular materials, *Archives of Metallurgy and Materials*, **50**, 3, 621-634

6. KUMAR R.S., MCDOWELL D.L., 2004, Generalized continuum modeling of 2-D periodic cellular solids, *Int. Journal of Solids and Structures*, **41**, 7399-7422

7. LAKES R.S., 1991a, Deformation mechanisms of negative Poisson's ratio materials: structural aspects, *Journal of Material Science*, **26**, 2287-2292

8. LAKES R.S., 1991b, Experimental micromechanics methods for conventional and negative Poisson's ratio cellular solids as Cosserat continua, *J. Engineering Materials and Technology*, **113**, 148-155

9. LAKES R.S., 1992, No contractile obligations, *Nature*, **358**, 713-714

10. LAKES R.S., 1993a, Advances in negative Poisson's ratio materials, *Advanced Materials*, **5**, 293-296

11. LAKES R.S., 1993b, Design considerations for negative Poisson's ratio materials, *ASME Journal of Mechanical Design*, **115**, 696-700

12. LAKES R.S., FRISS E.A., PARK J.B., 1988, Negative Poissons ratio for polymeric and metallic materials, *Journal of Material Science*, **23**, 4406-4414.

13. LAKES R.S., WITT R., 2002, Making and characterizing negative Poisson's ratio materials, *Int. Journal of Mechanical Engineering Education*, **30**, 50-58

14. MEHRABADI M.M., COWIN S.C., 1990, Eigentensors of linear anisotropic elastic materials, *Quarterly Journal of Mech. Appl. Math.*, **43**, 15-41

15. NEMAT-NASER S., HORI M., 1999, *Micromechanics*, 2nd edition, Elsevier

16. OSTROWSKA-MACIEJEWSKA J., RYCHLEWSKI J., 2001, Generalized proper states for anisotropic elastic materials, *Archives of Mechanics*, **53**, 4/5, 501-518

17. OVERAKER D.W., CUITINO A.M., LANGRANA N.A., 1998, Elastoplastic micromechanical modeling of two-dimensional irregular convex and nonconvex (Re-entrant) hexagonal foams, *Transactions of ASME*, **65**, 748-757

18. PIECHNIK S., 2003, *Wytrzymałość materiałów*, manual for students, Kraków

19. SMITH C.W., GRIMA J.N., EVANS K.E., 2000, A novel mechanism for generating auxetic behaviour in reticulated foams: missing rib foam model, *Acta Materialia*, **48**, 4349-4356

20. WARREN W.E., KRAYNIK A.M., 1988, The linear elastic properties of open-cell foams, *Journal of Applied Mechanics*, **55**, 341-346

Tytuł w j. polskim – proszę dopisać!!

Streszczenie

Streszczenie w j. polskim – proszę dopisać!!

Manuscript received November 13, 2008; accepted for print April 6, 2009